# Hadron-hadron interaction in a string-flip model of quark confinement. I. Meson-meson interaction

Makoto Oka
*Center for Theoretical Physics, Laboratory for Nuclear Science and Department of Physics, Massachusetts Institute of Technology, Cambridge, Massachusetts 02139*
(Received 20 August 1984)

The string-flip model of quark confinement is extended and applied to $q^2\bar{q}^2$ systems with color, spin, and flavor degrees of freedom. A realistic model for systems of two light mesons is constructed and the meson-meson interaction is investigated with the resonating-group method. Choosing the confinement strength for the confined ("hidden-color") state is discussed in detail. We find that the interaction in the confined state often produces two-meson bound states or low-lying sharp resonances. The $2^+$ two-vector-meson systems and the $K$-$\bar{K}$ interaction are studied in detail. The results are compared with those for other models and the possibility of observing "hidden-color" dominant resonances is discussed.

## I. INTRODUCTION

Recent development of perturbative and nonperturbative approaches to quantum chromodynamics (QCD) provides us with a fundamental understanding of hadron structure and interaction. For high-momentum-transfer phenomena (hard process), perturbative QCD is very successful, due to the asymptotic free nature of QCD. On the other hand, soft QCD processes are much less understood. There QCD is very complicated due to the color confinement. Although Monte Carlo calculation for lattice QCD is a promising nonperturbative approach, calculations done so far still have uncontrollable approximations. Furthermore, it seems rather complicated to apply it to multihadron systems.

Under these circumstances, many effective quark models for low-energy phenomena have been proposed. One of them is the quark potential model. An effective Hamiltonian for valence quarks is introduced. The interquark potential contains a long-range part, which confines the quarks in a color-singlet hadron, and a short-range spin-dependent interaction. The confining potential for quarks in a single hadron may be taken as the sum of a two-body force, i.e.,

$$V=\sum_{i<j} v(r_{ij}) , \tag{1.1}$$

where $v(r_{ij})$ is an infinitely rising function of the distance between the two quarks, $i$ and $j$, such as $v(r_{ij})\propto r_{ij}{}^n$ ($n=1$ or 2). Such effective Hamiltonians have succeeded remarkably well in explaining the low-lying hadron spectrum.[1,2]

This success leads one to try to understand multihadron systems with a similar model. A lot of work has been done in this context.[3–5] For hadron-hadron interaction, it was pointed out that exchange forces due to antisymmetrization of quarks are important and that the most reliable approach to the exchange force is the quark-cluster model.[5] The confining potential for multihadron systems which is appropriate for the quark-cluster model should satisfy the following conditions: (i) In a color-singlet hadron, the confining potential is reduced to the form (1.1) and confines the quarks, (ii) it guarantees the asymptotic separability of color-singlet hadrons, and (iii) it allows the exchange symmetry among the quarks (and among the antiquarks). The first two conditions guarantee a consistent treatment of single-hadron and multihadron systems. The third condition is necessary for a proper antisymmetrization, which is important in order to investigate the exchange forces between hadrons. The most conventional form which satisfies the above conditions is given by the sum of a color-dependent two-body potential,[6] i.e.,

$$V=-C\sum_{i<j}(\lambda_i\cdot\lambda_j)v(r_{ij}) , \tag{1.2}$$

where $\lambda_i$ denotes the color operator of the $i$th quark and the constant $C$ is determined by condition (i). This is a unique choice for the two-body potential with global color gauge invariance. A difficulty of the model, however, was pointed out by several authors,[7] that it gives a long-range attraction, called color van der Waals force, between two color-singlet hadrons, which seems to contradict experimental data on the nucleon-nucleon scattering.

Recently an alternative, called the string-flip model, was proposed[8] to avoid the color van der Waals force. The quark confinement is described in terms of a two-body potential $v$ (string), which is assumed to be the same as $v(r_{ij})$ in Eq. (1.1). In a multiquark system, strings connect the quarks according to a given configuration rule. The string configuration in a single hadron is obvious. The confining potential energy is given by Eq. (1.1). For a multihadron system the string configuration is determined as the shortest string (or lowest-energy) combination among all the possible combinations. This process gives us a many-body force, i.e., an $n$-body confining potential in an $n$-body system. One may easily imagine a picture of, for instance, the meson-meson interaction in this model. A system with two well-separated mesons has two strings. One of them makes a meson by connecting a quark 1 and an antiquark $\bar{1}$ and another connects 2 and $\bar{2}$. The quarks belonging to different mesons when well separated do not interact with each other at all and therefore no long-range (power-law) force appears. When the two mesons are put close to each other, the strings flip suddenly into another combination, i.e., 1-$\bar{2}$ and 2-$\bar{1}$, if the latter has shorter string length or lower confinement energy. This mechanism produces direct and exchange meson-meson interactions supplemented by the exchange symmetry. We wish to stress that for the single-meson (-hadron) system the string-flip model gives the same Hamiltonian as the two-body potential model. The single-hadron phenomenology therefore cannot distinguish them.

The string-flip model is similar to flux-tube models of quark confinement[9] and is expected to mimic the confinement mechanism in QCD. In fact, if confinement is related to a phase transition of the vacuum, color-electric flux tubes are produced instead of strings. The adiabatic approximation to the color-electric field gives us a configuration of the color flux tubes around quarks (color charges), which is represented by the string-flip model.

The color degree of freedom is important in the confinement mechanism. Only the color-singlet system exists in isolation, while the colored one is confined. The confining potential should depend on the color of the system. In Ref. 8, the authors proposed a colored string-flip potential model, which contains color projection operators onto the color-singlet component of subsystems. They pointed out that there is an ambiguity in choosing the strength of the confining force in the confined ("hidden-color") state without changing any property of the (color-singlet) hadron spectrum. The hidden-color state may have a very low energy and therefore may produce a bound or sharp resonance state due to the coupling with two-meson systems.[8] Such bound or resonance states are very new objects, never seen before because they are dominated by the hidden-color component.

The purpose of this paper is to investigate properties of the string-flip model in two-meson ($q^2\bar{q}^2$) systems by the quark-cluster-model approach. We concentrate on the behavior of systems with color and other internal degrees of freedom. A realistic model is proposed for the light-meson systems and is compared with the conventional two-body potential model.

This paper is organized as follows. The quark-cluster model for two-meson systems is given in Sec. II. Wave function and equation of motion of two-meson systems are presented.

In Sec. III we briefly review the string-flip model which incorporates no internal degrees of freedom for quarks. Even this simple model shows interesting behavior in two-meson systems which depends on the symmetry structure of the wave function. The internal degrees of freedom are expected to play important roles because they determine the orbital symmetry of the system.

Color is introduced in Sec. IV. We discuss ambiguities in choosing the colored string-flip model. The "colored" model taken here is slightly different from that in Ref. 8, although the role of the hidden-color state seems to be qualitatively the same. It is surprising that various different features are seen by changing the strength of the confining force in the hidden-color state, which does not affect the single-meson dynamics.

In Sec. V, we introduce spin and flavor and try to make a realistic model. A short-range spin-dependent interaction is also introduced in order to fit the low-lying meson spectrum. It is found that the various features seen in the colored model remain in the realistic model. We examine two particular cases where bound or sharp resonance states have a good chance to be experimentally observed. A possible interpretation of present candidates for $q^2\bar{q}^2$ resonances is discussed and compared with other models, such as the MIT bag model and the two-body potential model of confinement.

The conclusion appears in Sec. VI.

## II. WAVE FUNCTION, EQUATION OF MOTION FOR TWO-MESON SYSTEM

Let us consider a system with two quarks (1 and 2) and two antiquarks ($\bar{1}$ and $\bar{2}$). We take the Hamiltonian for this system as

$$H = K + V \,, \tag{2.1}$$

$$K = 4m + \frac{1}{2m}\sum_i {p_i}^2 - \frac{1}{2(4m)}\left[\sum_i p_i\right]^2 , \tag{2.2}$$

where we assume that the system is nonrelativistic and all the particles have the same mass $m$. We introduce the following coordinate system,[8] which is appropriate to discuss the two-meson scattering problem, i.e.,

$$\begin{aligned} R &= \tfrac{1}{4}(r_1 + r_2 + r_{\bar{1}} + r_{\bar{2}}) \,, \\ x &= \tfrac{1}{2}(r_1 + r_2 - r_{\bar{1}} - r_{\bar{2}}) \,, \\ y &= \tfrac{1}{2}(r_1 + r_{\bar{1}} - r_2 - r_{\bar{2}}) \,, \\ z &= \tfrac{1}{2}(r_1 + r_{\bar{2}} - r_{\bar{1}} - r_2) \,. \end{aligned} \tag{2.3}$$

The kinetic energy (2.2) is expressed in terms of the new coordinates (2.3) as

$$K = 4m + \frac{1}{2m}({p_x}^2 + {p_y}^2 + {p_z}^2) \,. \tag{2.4}$$

The center of mass $R$ of the total system is separated out because the potential $V$ is independent of $R$. The coordinate $x$ is always confined, i.e., $\Psi(x,y,z) \to 0$ as $x \to \infty$, for the $q^2$ system cannot be free from the $\bar{q}^2$. The other two, $y$ and $z$, can be free. The system has to have a definite symmetry under the exchange of the two quarks ($1 \leftrightarrow 2$), which means

$$\Psi(x,y,z) = +\Psi(x,z,y) \quad \text{(symmetric)} \,, \tag{2.5}$$

or

$$\Psi(x,y,z) = -\Psi(x,z,y) \quad \text{(antisymmetric)} \,. \tag{2.6}$$

Thus the general wave function of the system is written as

$$\Psi(x,y,z) = \sum_m [\phi_m(x,y)\chi_m(z) \pm \phi_m(x,z)\chi_m(y)] \,, \tag{2.7}$$

where $\chi_m(z)$ represents a relative wave function in a two-meson channel $m$ and $\phi_m(x,y)$ denotes the corresponding internal function.

The resonating-group method[10] (RGM) is employed to solve the bound state and the scattering problem of two mesons. Assuming that the internal wave function $\phi_m(x,y)$ is known, an equation for $\chi(R)$ is derived from the Schrödinger equation as

$$\begin{aligned} 0 &= \int \phi_m^\dagger(x,y)\delta(z-R)(H-E)\Psi(x,y,z)dx\,dy\,dz \\ &= \sum_{m'} \int [H_{mm'}(R,R')-EN_{mm'}(R,R')]\chi_{m'}(R')dR' \ . \end{aligned} \tag{2.8}$$

Here the integral kernels $H_{mm'}(R,R')$, or Hamiltonian kernel, and $N_{mm'}(R,R')$, normalization kernel, are split into direct and exchange parts, i.e.,

$$H_{mm'}(R,R')=H^D_{mm'}(R)\delta(R-R')\pm H^{\rm ex}_{mm'}(R,R') \ , \tag{2.9}$$

$$N_{mm'}(R,R')=\delta_{mm'}\delta(R-R')\pm N^{\rm ex}_{mm'}(R,R') \tag{2.10}$$

with

$$\begin{aligned} H^D_{mm'}(R) &= \int \phi_m^\dagger(x,y)H\phi_m(x,y)dx\,dy \\ &= E_{\rm in}-\frac{1}{2\mu}\nabla_R{}^2+V^D_{mm'}(R) \ , \end{aligned} \tag{2.11}$$

$$\begin{aligned} H^{\rm ex}_{mm'}(R,R') = \int & \phi_m^\dagger(x,y)\delta(R-z)H\phi_{m'}(x,z) \\ & \times\delta(R'-y)dx\,dy\,dz \ , \end{aligned} \tag{2.12}$$

$$\begin{aligned} N^{\rm ex}_{mm'}(R,R') &= \int \phi_m^\dagger(x,y)\delta(R-z)\phi_{m'}(x,z) \\ &\qquad \times\delta(R'-y)dx\,dy\,dz \\ &= \int \phi_m^\dagger(x,R')\phi_{m'}(x,R)dx \ . \end{aligned} \tag{2.13}$$

Equation (2.8), a set of coupled integrodifferential equations for $\chi_m(R)$, is solved under appropriate boundary conditions for bound-state and scattering problems. A variational method[11] is employed to solve Eq. (2.8) numerically, where the relative wave function $\chi_m(R)$ is expanded as a sum of locally peaked Gaussians.

The set of relative wave functions $\{\chi_m(R)\}$ may not be uniquely determined because in some cases particular sets of functions $\{\chi_m^{(n)}(R)\}$ ($n=1,2,\ldots$) vanish the total wave function (2.7) due to the (anti)symmetrization. Each $\{\chi_m^{(n)}(R)\}$ satisfies

$$\sum_{m'} \int N_{mm'}(R,R')\chi_{m'}^{(n)}(R')dR'=0 \tag{2.14}$$

and is known as a "Pauli-forbidden" state. To determine $\{\chi_m(R)\}$ uniquely, we need an additional condition,

$$\sum_m \int \chi_m(R)\chi_m^{(n)}(R)dR=0 \quad \text{for all } n \ . \tag{2.15}$$

The nonuniqueness of $\{\chi_m(R)\}$ and the existence of Pauli-forbidden states play important roles in the two-meson interaction.[12]

Any totally color-singlet $q^2\bar{q}^2$ state can be expressed as Eq. (2.7), i.e., an infinite sum of cluster states with two *color-singlet* mesons.[13] In Eq. (2.7), the index $m$ runs over all the possible ground and excited internal states of two mesons. We, however, have to truncate the sum over $m'$ to solve Eq. (2.8) numerically. One or a few lower eigenstates are taken into account in the actual calculation. The convergence of the truncation is a dynamical problem. We will find in Sec. III that for the colorless model the single-channel approximation is little affected by the coupling of excited internal states for energies up to the excitation threshold.

The situation changes when one considers the color degree of freedom. Two color-octet $q\bar{q}$ systems can be combined into a totally color-singlet state as

$$\Psi_8(x,y,z)=\phi_8(x,y)\chi_8(z)\pm\phi_8(x,z)\chi_8(y) \ , \tag{2.16}$$

where $\phi_8(x,y)$ denotes a totally color-singlet state with two color-octet $q\bar{q}$ systems, i.e.,

$$\phi_8(x,z)=[\varphi_8(1,\bar{1})\varphi_8(2,\bar{2})]_1 \ . \tag{2.17}$$

$\Psi_8$ is often referred to as a hidden-color[14] (HC) state since the colored $q\bar{q}$ system must always be confined and is hidden, i.e., $\chi_8(z)\to 0$ when $z\to\infty$ in Eq. (2.16). In principle, we do not need to introduce any HC state explicitly in the RGM calculation, because $\Psi_8$ is equivalent to a sum of cluster states with two color-singlet mesons. The truncation of internal states of the meson, however, leads to a problem of slow convergence if some HC states are dynamically favored. When the color degree of freedom is introduced in the string-flip model in Sec. IV, we will find that the HC states can couple so strongly that we need to consider them explicitly. The lowest orbital state is taken as $\phi_8$ in the RGM calculations and the effect of its coupling will be investigated.

As is well known, the two-body confining potential (1.2) gives rise to a long-range color van der Waals force. It comes from the coupling of color-dipole polarized states, which is again equivalent to a sum of the two color-singlet meson states with high orbital excitations. In the actual calculation, the color van der Waals force is effectively eliminated by the technical approximation of truncating the sum in Eq. (2.7) to the low-lying meson states. To justify this truncation procedure, the quark Hamiltonian with the two-body confining potential (1.2) should be considered as an effective one in a limited space of low-lying internal states for the mesons in the RGM wave function.

## III. COLORLESS MODEL

Let us briefly discuss a simple model which has no internal degrees of freedom such as color, spin, and flavor. It only incorporates the string-flip mechanism proposed in Ref. 8. This model has already been studied in detail in Ref. 8, where the equation of motion is solved quasi-analytically. We confirm their results using the variational method in solving the resonanting-group equation (2.8) and present a few details in order to make further discussion clear.

The Hamiltonian proposed in Ref. 8 reads

$$H = K + V = h_x + h_{yz} , \tag{3.1}$$

$$K = 4m + \frac{1}{2m}\sum_i p_i{}^2 - \frac{1}{8m}\left[\sum_i p_i\right]^2$$
$$= 4m + \frac{1}{2m}(p_x{}^2 + p_y{}^2 + p_z{}^2) , \tag{3.2}$$

$$V = v(x) + V(y,z) , \tag{3.3}$$

with

$$h_x = \frac{1}{2m}p_x{}^2 + v(x) , \tag{3.4}$$

$$h_{yz} = 4m + \frac{1}{2m}(p_y{}^2 + p_z{}^2) + V(y,z) , \tag{3.5}$$

$$v(x) = 2v_0 x^2 = \tfrac{1}{2}m\omega^2 x^2 , \tag{3.6}$$

$$V(y,z) = \min(v(y), v(z)) = 2v_0 \min(y^2, z^2) . \tag{3.7}$$

Here harmonic confinement is chosen for simplicity and one sees that the variable $x$ is decoupled as a harmonic-oscillator Hamiltonian whose solution is known. At large $y\,(>z)$ the Hamiltonian $h_{yz}$ is reduced to

$$h_{yz} = 4m + \frac{1}{2m}p_y{}^2 + \left[\frac{1}{2m}p_z{}^2 + \frac{m}{2}\omega^2 z^2\right] , \tag{3.8}$$

which is the sum of a free $y$ motion (i.e., two mesons move freely) and a harmonic oscillator for $z$, which is the internal coordinate of the mesons with the additional variable $x$.

The variational method to solve the resonating-group equation is applied for $h_{yz}$. We carry out the single-channel calculation, where the internal state of the meson is restricted to the $0s$, and the coupled-channel calculation with the $1s$ excited state for the variable $y$. We summarize the results as follows. (1) The $S$-wave scattering phase shift for the antisymmetrized ($A$) scattering problem, where the quarks (antiquarks) are antisymmetrized in the orbital space, behaves like that for the scattering from a hard sphere with the radius $R_0 \simeq 1.5b$ [$b = (4mv_0)^{-1/4}$]. The corresponding relative wave function, $\chi(R)$ has a node almost independent of the energy at $R = R_0$. Such behaviors are well known to come from the existence of a Pauli-forbidden state, which is the relative $0s$ motion in the present case.[12] (2) A strong attractive force is indicated between the two mesons for the symmetrized ($S$) scattering problem. There exists a shallow bound state whose binding energy is 0.04 $\hbar\omega$. The $S$-wave scattering phase shift shows a sharp resonance just below the threshold energy for internal excitation. The resonance is a "virtual" bound state in the excited channel and the coupling with the ground-state channel is very weak. (3) Effect of the channel coupling is almost negligible except for the $S$ scattering at the vicinity of the resonance. (4) The variational method employed here is found to be safely applied to such sharp resonances in the scattering problem.

## IV. COLORED MODEL

In the colorless model discussed in the previous section, we found that the effective interaction between mesons is dictated by the symmetry structure of the orbital wave function. The exchange interaction induced by the antisymmetrization gives a strong hard core like repulsion, while that by the symmetrization gives an attraction which has a bound state. It is expected that introduction of internal degrees of freedom for the quark is important because the orbital symmetry structure of the system is determined by that of the internal degrees of freedom. Pauli-forbidden states no longer exist in the single-channel approximation with the internal degrees of freedom, though they may play a role in the coupled-channel formulation as is seen later.

It is essential to introduce the color since the quark is believed to be confined in a color-singlet system. We seek a model which confines all the color-nonsinglet subsystems including a single quark while it allows free motion for the color-singlet hadrons. Extending the string-flip model to include color, we confront ambiguities. From the single-meson spectroscopy, we can learn the string potential for the color-singlet $q\bar{q}$ system. For the colorless model, the same $q\bar{q}$ potential should appear also in the $q^2\bar{q}^2$ system, because any $q\bar{q}$ subsystem can be made free. In the colored model, however, one can arbitrarily choose the confining force for the color-nonsinglet $q\bar{q}$ system. Change of the confining potential for color-nonsinglet subsystems does not affect the single-meson spectrum, while it changes the meson-meson interaction.

Here we try a simple extension of the original string-flip model by introducing a color projection operator as follows:

$$V = \frac{2v_0}{\rho}\{2x^2 + y^2 + z^2 - \theta(y^2 - z^2)[(2-\rho)x^2 + y^2 + (1-\rho)z^2]P_y - \theta(z^2 - y^2)[(2-\rho)x^2 + z^2 + (1-\rho)y^2]P_z\} , \tag{4.1}$$

with

$$P_y = P_{1\bar{1}}P_{2\bar{2}} , \tag{4.2}$$

$$P_z = P_{1\bar{2}}P_{2\bar{1}} , \tag{4.3}$$

where $P_{i\bar{j}}$ is the projection operator onto the color-singlet system for $i$ and $\bar{j}$. Suppose that $y > z$ and $P_y = 1$ ($1\bar{1}$ and $2\bar{2}$ are color singlet), then

$$V = 2v_0(x^2 + z^2) = v_0[(r_1 - r_{\bar{1}})^2 + (r_2 - r_{\bar{2}})^2] , \tag{4.4}$$

which gives the internal potential. If $P_y = 0$ and still $y > z$, which corresponds to a hidden-color (HC) state with large separation, the potential reads

$$V=\frac{2v_0}{\rho}(2x^2+y^2+z^2)$$
$$=\frac{v_0}{\rho}[(r_1-r_{\bar{1}})^2+(r_2-r_{\bar{2}})^2+(r_1-r_{\bar{2}})^2+(r_2-r_{\bar{1}})^2]\ , \tag{4.5}$$

which confines all the particles. The parameter $\rho$ is introduced in order to change the strength of the HC confinement. If $\rho$ is greater than 2, then the confining force per particle is weaker than that in a color-singlet meson. We therefore expect that for a large $\rho$ the energies of HC states become lower and the explicit introduction of the HC state is necessary to avoid the slow convergence of the truncation in the two-meson states. If $\rho$ is less than 2, HC states are pushed up by the confining potential. Because changing $\rho$ is entirely independent of the dynamics of the single meson, we obtain many different models for $q^2\bar{q}^2$ systems which have equivalent meson spectra.

We may determine the value of $\rho$ by the long-distance behavior of the confining force. The global color gauge invariance relates the confining strength between two color-octet objects to that in a color-singlet meson. In fact, using matrix elements of $F_i\cdot F_j$, where $F_i$ is a color SU(3) generator, we obtain $\rho=\frac{8}{9}$. However, we here consider $\rho$ as a free parameter with the following reason. The global gauge invariance or the potential proportional to $F_i\cdot F_j$ gives us a repulsive (anti)confinement in the color-octet $q\bar{q}$ system, which is not realistic. Our model has an attraction there and the energy for HC states is different from the $F_i\cdot F_j$ potential model. In the present investigation, the energy difference between color-singlet cluster states and HC states in the short-distance region is important and therefore the value $\rho=\frac{8}{9}$ determined by the long-range behavior may not be relevant.

The form of the potential (4.1) is not a unique extension of the colorless model. One may also introduce the $qq$ and $\bar{q}\,\bar{q}$ confining force for HC states, which is not considered here as is seen from Eq. (4.5). One such potential is chosen in Ref. 8. They took a special choice for the $qq$ and $\bar{q}\,\bar{q}$ confining potential which enables them to decouple the $x$ coordinate completely from the others. By this special assumption, they could solve the meson-meson scattering problem quasianalytically. The variable $x$ is no longer decoupled in our choice of the confining potential (4.1).

Let us first consider the antisymmetrized ($A$) scattering where the quarks are antisymmetrized in the color-orbital space. Figure 1 shows the $S$-wave $A$-scattering phase shifts in the single-channel calculation, which only takes the ground-state $0s$ meson into account. We take several values of $\rho$ as typical ones. It is at first surprising that resonancelike structures are seen being highly dependent on $\rho$ even without the HC coupling. This behavior of the phase shifts is consistent with that of the direct potential $V^D(R)$ (Fig. 2), which depends strongly on $\rho$. Such $\rho$ dependence can be understood by knowing that in general an antisymmetrized two-(color-singlet)-meson state is not orthogonal to the HC cluster states. For instance, the two-meson state with $0s$ relative motion is also expressed as a HC state, i.e.,

$$\mathscr{A}[\varphi_1(1,\bar{1})\varphi_1(2,\bar{2})\chi(0s)]\propto\mathscr{A}[\varphi_8(1,\bar{1})\varphi_8(2,\bar{2})\chi(0s)]\ , \tag{4.6}$$

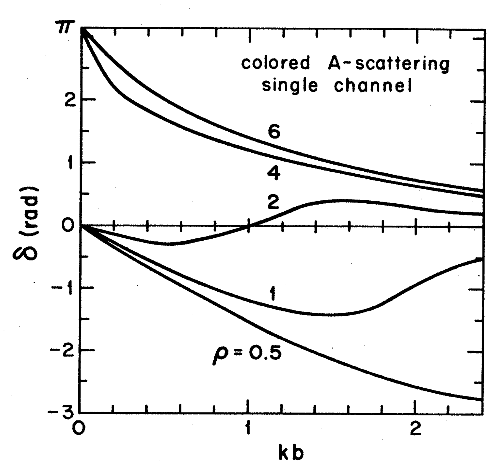


FIG. 1. The $A$-scattering phase shifts for the colored model with several values of $\rho$ obtained by the single-channel calculation. $k$ denotes the relative momentum and $b=(1/m\omega)^{1/2}$. The inelastic threshold corresponds to $kb=2$, i.e., the threshold energy $E_{\text{th}}=2\hbar\omega$. There exists a bound state for $\rho=4.0$ (6.0), the binding energy of which is $0.014\hbar\omega$ $(0.11\hbar\omega)$.

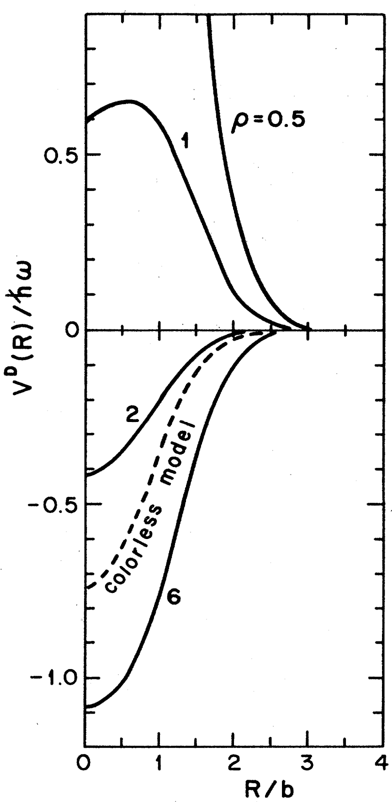


FIG. 2. The direct potential $V^D(R)$ between the two mesons for the colored model (solid curves) and for the colorless one (dashed curve). $b=(1/m\omega)^{1/2}$.

where $\mathscr{A}$ stands for the antisymmetrization operator and both the orbital parts of $\varphi_1$ (color-singlet meson) and $\varphi_8$ (color-octet $q\bar{q}$) are taken as $0s$ states. The energy of the HC state is very sensitive to the parameter $\rho$. The two-meson state, therefore, feels an attractive force in the interaction region via the HC component of the wave function, if $\rho$ is large. We will see in a moment that the lowest bound state or resonance, the energy of which is highly dependent on $\rho$, has a wave function very similar to Eq. (4.6).

HC states with excited relative motion are independent of the cluster state with two ground-state mesons. The resonating-group-method (RGM) Eq. (2.8) is solved including both the $0s$ meson and the $0s$ color-octet $q\bar{q}$ systems in the wave function (2.7). Figure 3 shows the $A$-scattering phase shifts for several choices of $\rho$. A lot of sharp resonances are observed, which are considered to come from the coupling of two-meson scattering states to discrete levels of the HC confined channel, because they have not been seen in the single-channel calculation. In order to examine the structure of the resonances, we define color symmetry basis states by

$$|a\rangle=(\tfrac{1}{3})^{1/2}|(1,\bar{1})_8(2,\bar{2})_8\rangle-(\tfrac{2}{3})^{1/2}|(1,\bar{1})_1(2,\bar{2})_1\rangle\ , \tag{4.7}$$

$$|s\rangle=(\tfrac{2}{3})^{1/2}|(1,\bar{1})_8(2,\bar{2})_8\rangle+(\tfrac{1}{3})^{1/2}|(1,\bar{1})_1(2,\bar{2})_1\rangle\ . \tag{4.8}$$

The color-antisymmetric state $|a\rangle$ belongs to a $\mathbf{3}^*$ representation of the color SU(3) for the two quarks and therefore belongs to a $\mathbf{3}$ representation for the antiquarks. Orbital wave functions coupled to $|a\rangle$ should be symmetric. On the contrary, $|s\rangle$ belongs to the color-symmetric $\mathbf{6}$ representation and couples to the antisymmetric orbital state. As a result, we expect the $|a\rangle$ coupling has lower energy than $|s\rangle$ for the $A$ scattering. The $|s\rangle$ coupling has a Pauli-forbidden state, which causes the degeneracy relation (4.6). Because the relative $0s$ motion in $|s\rangle$ is not allowed by the Pauli principle, one expects that the lowest bound or resonance state will have a nodeless relative wave function in the $|a\rangle$ coupling. The explicit relative wave function confirms the above. The phase and the ratio of the color-singlet and color-octet components are found to be almost identical to Eq. (4.7). The HC component is favored by the confining potential for the higher excited resonances. There the color-symmetric $|s\rangle$ coupling is mixed to $|a\rangle$ so as to suppress the color-singlet component of the wave function in the internal region. As a result, the coupling to the continuum state becomes weak and the resonances become very sharp. The widths of the resonances seem narrower for the higher resonances, because HC wave functions with higher excited relative motion have small overlap with two-meson scattering wave functions.

The coupled-channel calculation is carried out including the $(1s)_x$ and $(1s)_y$ excited two-meson states in order to see whether a threshold resonance, which appears in the symmetrized scattering problem in the colorless model, exists. We found no new sharp resonance coming from the coupling of the orbitally excited mesons for $\rho=1$ and 4 (Fig. 4).[15] The resonances for $\rho=4$ observed before remain at almost the same positions, although the reso-

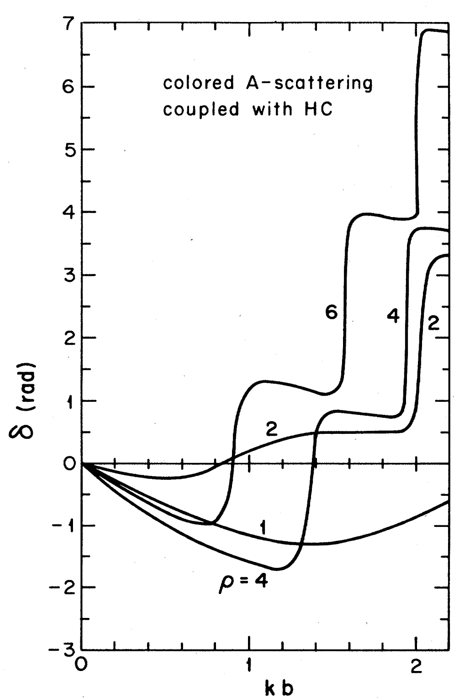


FIG. 3. The $A$-scattering phase shifts for the colored model obtained by the coupled-channel calculation. A bound state with the binding energy $0.21\hbar\omega$ ($0.49\hbar\omega$) exists for $\rho=4.0$ (6.0).

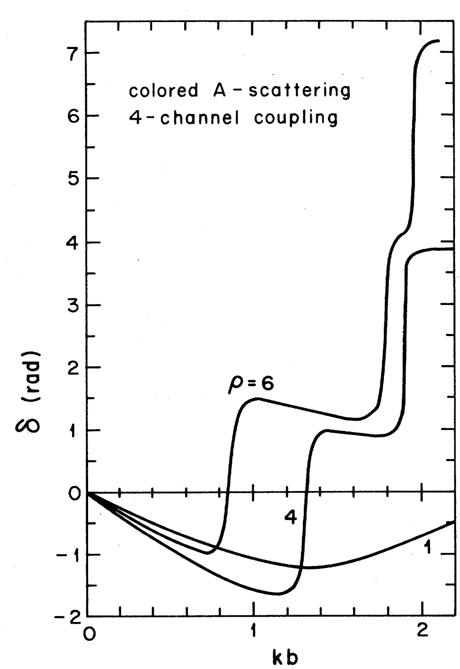


FIG. 4. The $A$-scattering phase shifts obtained by the four-channel coupling calculation. The inelastic threshold, $E_{\text{th}}=2\hbar\omega$, corresponds to $kb=2$. The binding energy becomes $0.24\hbar\omega$ ($0.54\hbar\omega$) for $\rho=4.0$ (6.0).

nance wave functions tell us that the $(1s)_x$ excited state mixes significantly for the second resonance. The resonance structure for $\rho=6$ is affected near threshold. The second and the third resonances are significantly shifted due to the mixing of the orbitally excited states.

The role of the color-symmetric $|s\rangle$ and the antisymmetric $|a\rangle$ states are interchanged for the symmetrized ($S$) scattering. Figure 5 shows the $S$-wave scattering phase shifts for the $S$ scattering. One sees that the resonances come out at almost the same energies as those for the $A$ scattering, while the resonance widths are much larger. In this case the color-symmetric $|s\rangle$ coupling corresponds to the symmetric orbital state and the lowest bound or resonance state has a nodeless relative wave function which belongs to $|s\rangle$. The higher resonances belong mainly to $|s\rangle$ again and their widths, which show the strength of the coupling of the HC discrete level with two-meson continuum state, are larger than those for the $A$ scattering, as is expected from Eqs. (4.7) and (4.8). It, however, gives threshold resonances for $\rho=4$ and 6. The resonance wave function contains a large portion of the $x$-excited channel. The effect of the couplings to the orbitally excited states is again small for the lower energies.

We have employed only the $0s$ color-octet $q\bar{q}$ state so far. A question may arise whether this is a good approximation.[6] We have to check whether HC low-lying states are well approximated by the wave function (2.16). For that purpose the size parameter $b_8$ for the colored $q\bar{q}$ system is changed from that for the meson, $b=(1/m\omega)^{1/2}$. We seek the optimum value of $b_8$ for each value of $\rho$ by searching for the minimum of the lowest HC state (2.16). (We get a discrete spectrum in this space because HC states are always confined.) The calculated $A$-scattering phase shifts for the optimal value of $b_8$ shows us that the qualitative features are not affected for a small $\rho$, although the position of the resonances, which almost coincide with the eigenenergies stated above, are slightly shifted to lower energies. For $\rho=4$, we find a new resonance (at $k=1.90/b$) besides the shifts of the resonances observed before. The resonance wave function belongs mainly to the color-symmetric $|a\rangle$ coupling. The width is a little larger than the widths for the color-antisymmetric resonances, because the color-symmetric coupling (4.8) contains more color-singlet components. We conclude that the present truncation of the $q\bar{q}$ states in the RGM wave function (2.7) is appropriate at low energies.

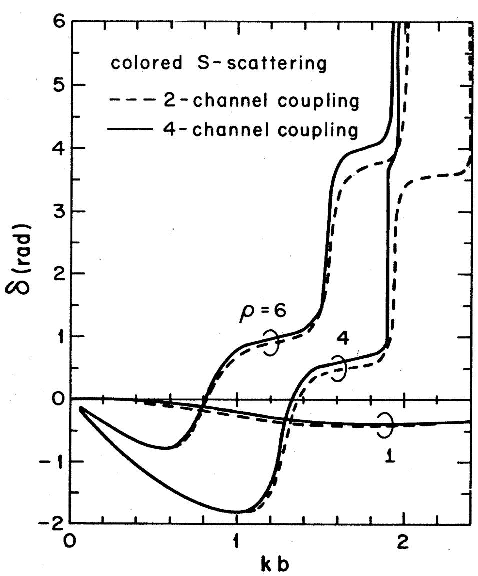


FIG. 5. The $S$-scattering phase shifts for the colored model. The dashed curves show the results obtained by the two-channel (ground-state and HC) coupling calculation and the solid ones by the full four-channel coupling calculation. The binding energy of the bound state for $\rho=4.0$ (6.0) is $0.12\hbar\omega$ ($0.30\hbar\omega$).

## V. REALISTIC MODEL

In the previous section, we see that the colored model shows us various features of the meson-meson interaction. The bound and resonance states, which appear for large values of the parameter $\rho$, are new. They are dominated by a cluster state with two color-octet $q\bar{q}$ systems and thus seem like hidden-color (HC) bound states. The resonances are very sharp due to weak coupling to continuum states of two color-singlet mesons. It is very interesting to investigate such hidden-color dominated resonances in a more realistic model. We wish to stress again the role of the parameter $\rho$. There is no way to determine $\rho$ in a phenomenological analysis of the single-meson system, because the $q\bar{q}$ Hamiltonian is independent of $\rho$. Instead, $\rho$ determines the confinement strength for the HC state and thus the extent of the HC coupling in the two-meson or $q^2\bar{q}^2$ system. Only two-meson phenomenology may distinguish different values of $\rho$. We will estimate the reasonable range of $\rho$ by comparing the results of the calculation with present candidates for $q^2\bar{q}^2$ resonances.

Now we introduce spin and flavor and construct a realistic model for the light-quark ($u$, $d$, and $s$) systems. We also introduce a short-range interaction between the quarks and antiquarks. Much work has been done on the low-lying meson and baryon spectra in the potential quark model.[1,2] Here the potential consists of a confining force and a spin-dependent short-range interaction. A well known form of the latter is the one-gluon-exchange potential,[2] which does a good job on the fine structure of the spectrum. In particular, the color-magnetic interaction, i.e.,

$$\sum(\lambda_i\cdot\lambda_j)(\sigma_i\cdot\sigma_j)f(r_{ij}) ,$$

is important in explaining detail structures of the spectrum and the decay properties. Here we wish to use a more general form of the short-range interaction,

$$V_{\rm SR}=\sum_{i<j}(\lambda_i\cdot\lambda_j)[f_0\exp(-\alpha_f r_{ij}^2) - g_0(\sigma_i\cdot\sigma_j)\exp(-\alpha_g r_{ij}^2)] , \quad (5.1)$$

for simplicity. We will call the first (second) term the color-electric (color-magnetic) interaction. The color-magnetic term breaks SU(6) symmetry and therefore causes the splitting of the pseudoscalar and vector mesons. The four parameters $f_0$, $g_0$, $\alpha_f$, and $\alpha_g$ are chosen so as to fit the meson spectrum.

We employ the nonrelativistic kinetic energy (3.2) with effective quark mass $m_q$. We stress here that the nonrelativistic quark Hamiltonian is an effective one which explains the observed meson spectrum. The kinetic-energy term cannot be investigated separately from the interaction and is not taken to be an approximation of a relativistic one. The remarkable success of the nonrelativistic potential model in explaining low-energy hadron properties suggests the effectiveness of the Hamiltonian. An advantage of the model is that the symmetry structure of the hadron is shown very clearly. In multihadron problems, the role of the internal symmetry of the system is very important and therefore the investigation by the use of the nonrelativistic model is preferable. There is another advantage of the nonrelativistic model: The center-of-mass coordinate of the hadron is separated exactly from the internal coordinates, which is again important in studying hadron-hadron problems.

The internal wave function of the ground-state meson is approximated by that of a harmonic oscillator $0s$ state with the size parameter $b$, i.e.,

$$\varphi(r_{q\bar{q}})=\mathcal{N}\exp(-r_{q\bar{q}}{}^2/4b^2)\ .$$

We obtain the masses of the pseudoscalar ($P$) and the vector mesons ($V$) for the Hamiltonian, which consists of the kinetic energy (3.2), the colored confining potential (4.1) and $V_{\rm SR}$ (5.1), as

$$\text{Mass of }\begin{bmatrix}P\\V\end{bmatrix}=m_q+m_{\bar{q}}+C+\left[\frac{2v_0}{\mu}\right]^{1/2}\frac{3}{4}\left[\frac{1}{(8\mu V_0)^{1/2}b^2}+(8\mu V_0)^{1/2}b^2\right]-\frac{16}{3}\left[f_0(1+2\alpha_f b^2)^{-2/3}+\begin{bmatrix}+3\\-1\end{bmatrix}g_0(1+2\alpha_g b^2)^{-2/3}\right], \tag{5.2}$$

where $\mu$ is the reduced mass. A constant $C$ is introduced to fit the absolute value of the meson mass. Note that the constant shift does not affect meson-meson dynamics. The size parameter $b$ is taken so as to minimize the mass (5.2) for each meson.[17] The parameters are fixed to fitting the experimental values of the masses of $\rho(\omega)$, $K$, $K^*$, and $\phi$ with the assumption of $m_{u,d}=300$ MeV and $m_s=500$ MeV. Table I gives a parameter set and the masses and the root-mean-square (rms) radii of the low-lying mesons. Values fitted to the experimental ones are indicated by asterisks. Note that we do not fit the pion mass because it is too light to be regarded as a nonrelativistic bound state. We assume that $g_0$ is independent of the quark mass and find that the color-electric term can be set to zero, i.e., $f_0=0$.

The conventional two-body confining potential, i.e.,

$$V_{\rm two}=-\tfrac{3}{16}v_0\sum_{i<j}(\lambda_i\cdot\lambda_j)r_{ij}{}^2\ , \tag{5.3}$$

is also considered instead of (4.1) in order to compare with the string-flip model. Equation (5.3) is totally equivalent to (4.1) for the color-singlet meson ($q\bar{q}$) spectrum.

Let us consider the two-meson system composed of the light ($u$, $d$, and $s$) quarks (and antiquarks). We have a pseudoscalar [$\pi$, $\eta_0\equiv(u\bar{u}+d\bar{d})/\sqrt{2}$, $K$, $\bar{K}$, and $\eta_s\equiv s\bar{s}$] and a vector ($\omega$, $\rho$, $K^*$, $\bar{K}^*$, and $\phi$) nonet for the ground states. Since the Hamiltonian is independent of the isospin, $\pi$ and $\eta_0$ ($\rho$ and $\omega$) are degenerate. The two-quark ($q^2$) states are classified by their flavor symmetry (Table II): we use the notation $A$ for the $q^2$ state with the $\mathbf{3}^*$ representation of the flavor SU(3) and $B$ with $\mathbf{6}$. $A$ ($B$) can couple with the symmetric (antisymmetric) color-spin-orbital wave function. In general, the orbital symmetric states, $A_{0a}$, $A_{1s}$, $B_{1a}$, and $B_{0s}$, are dynamically favored, while the antisymmetric ones will produce a Pauli-forbidden state in the $q^2\bar{q}^2$ system. By the use of the notation $A$ and $B$, the $q^2\bar{q}^2$ systems are classified as in Table III. The nonstrange sector of $B\bar{B}$ contains $I=0,1,2$ states, which are again degenerate. Combinations marked with asterisks are made from the symmetric orbital states. It is also noted that the combinations of different orbital symmetry, parenthesized in Table III, are

TABLE I. The parameters of the realistic model and the masses (in MeV) and the root-mean-square (rms) radii (in fm) of the low-lying mesons. Values fitted to experiment are indicated by asterisks.

| | | |
|---|---|---|
| $m_{u,d}$ | (MeV) | 300 |
| $m_s$ | (MeV) | 500 |
| $v_0$ | (MeV/fm$^2$) | 488 |
| $f_0$ | (MeV) | 0 |
| $\alpha_f{}^{-1/2}$ | (fm) | |
| $g_0$ | (MeV) | 120 |
| $\alpha_g{}^{-1/2}$ | (fm) | 3.95 |
| $\hbar\omega_{u,d}$ | (MeV) | 503 |
| $\hbar\omega_s$ | (MeV) | 390 |
| $\pi$ ($\eta_0$) | mass | 430 |
| | rms radius | 0.35 |
| $\rho$ ($\omega$) | mass | 769* |
| | rms radius | 0.47 |
| $K$ | mass | 496* |
| | rms radius | 0.32 |
| $K^*$ | mass | 897* |
| | rms radius | 0.45 |
| $\eta_s$ | mass | 520 |
| | rms radius | 0.27 |
| $\phi$ | mass | 1018* |
| | rms radius | 0.42 |

TABLE II. The classification of $q^2$ system. $A$'s couple to the symmetric [2] spin-color-orbit state, while $B$'s to the antisymmetric [11] one.

| | Flavor | Color | Spin | Orbital |
|---|---|---|---|---|
| $A_{0a}$ | $3^*$[11] | $3^*$[11] | 0 | [2] |
| $A_{1a}$ | $3^*$[11] | $3^*$[11] | 1 | [11] |
| $A_{0s}$ | $3^*$[11] | 6[2] | 0 | [11] |
| $A_{1s}$ | $3^*$[11] | 6[2] | 1 | [2] |
| $B_{0a}$ | 6[2] | $3^*$[11] | 0 | [11] |
| $B_{1a}$ | 6[2] | $3^*$[11] | 1 | [2] |
| $B_{0s}$ | 6[2] | 6[2] | 0 | [2] |
| $B_{1s}$ | 6[2] | 6[2] | 1 | [11] |

not relevant for the $S$-wave cluster state with two ground-state mesons.

Table IV shows the classification of nonstrange two-meson states in terms of the symmetry basis given in Table III. It should be noted here that the states $A\bar{A}$, $B\bar{B}$, and $[A\bar{B},B\bar{A}]_{\pm}$ become the eigenchannels of the Hamiltonian instead of the physical two-meson states. The unitary transform between the two is given by

$$\begin{bmatrix} A\bar{A} \\ B\bar{B} \end{bmatrix} = \begin{bmatrix} \frac{1}{2} & \sqrt{3}/2 \\ \sqrt{3}/2 & -\frac{1}{2} \end{bmatrix} \begin{bmatrix} M_0 M_0 \\ M_1 M_1 \end{bmatrix} \tag{5.4}$$

for $I^G=0^+$, for instance, where $M_I$ stands for a meson with isospin $I$. The eigenchannel $A\bar{A}$ ($B\bar{B}$) couples to the symmetric(antisymmetric) color-spin-orbital states.

In order to compare results of the calculation with experimental data, we have to notice several limitations of the present model. First of all, neither the annihilation nor the creation of the quark-antiquark pair is taken into account. As a result, the ground-state vector meson, $V$($\rho$, $\omega$, etc.), becomes a stable particle. The $q^2\bar{q}^2$ resonances may only decay into two-meson states and thus the other decay modes are neglected. We also neglect the two-meson interaction coming via an annihilation process. In fact, it dominates in some particular channels, such as $P$-wave $\pi\pi$ with $I=1$, where the annihilation process is apparently important due to the existence of the $\rho$ resonance. Introduction of the $q\bar{q}$ annihilation and production processes would be necessary to make a more realistic model and to treat two-meson channels dominated by single-meson resonances. We also have to note that the pion cannot be treated realistically, as was stated above. One therefore should not consider the $\pi\pi$ interaction seriously in this model, although most of the experimental data for two mesons is for $\pi\pi$.

Here we mainly study the following two cases: (1) $S$-wave spin-2 ($L=0$, $S=2$, $J^P=2^+$) states of two nonstrange vector mesons both in the $A\bar{A}$ and $B\bar{B}$ flavor symmetry, and (2) $S$-wave spin-0 ($L=0$, $S=0$, $J^P=0^+$) $K$-$\bar{K}$ states. The former, $(VV)_{S=2}$ scattering problem, is chosen because bound states and resonances, if any, may be observed experimentally. Due to the Okubo-Zweig-Iizuka (OZI) rule, the $2^+$ $q^2\bar{q}^2$ states decay only into two vector mesons in zeroth order.[18,19] The resonances near threshold are expected to be observed in the $\gamma\gamma\to\rho\rho$ experiment, for instance. The symmetry structure of the system is as simple as that of the colored model because all the spins of the quarks and antiquarks are aligned and each eigenchannel, $A\bar{A}$ or $B\bar{B}$, has a definite isospin symmetry. It is expected that the coupling of the HC channel, $(V_8V_8)_{S=2}$, will have a significant influence for a large $\rho$. The resonating-group method (RGM) calculation is carried out for the $S$-wave $(VV)_{S=2}$ scattering. Three different confining potentials are tested: (T) two-body confinement, (S1) string flip with $\rho=1.0$, and (S6) string flip with $\rho=6.0$ as an extreme case.

Figure 6 shows the $S$-wave scattering phase shifts for the $B\bar{B}$ scattering, which corresponds to the antisymmetrized scattering in the previous colored model. We summarize the results as follows. (1) A strong repulsion is indicated between two mesons for the model (S1). The phase shift is very similar to that for the colored model. The HC channel, $(V_8V_8)_{S=2}$, couples weakly and no resonance structure is seen up to 1 GeV. (2) A bound state with binding energy 374 MeV is predicted for the model (S6). The phase shift shows several sharp resonances. The structures of the bound and resonance states are again very similar to those for the colored model. The color-

TABLE III. The classification of the $S$-wave $q^2\bar{q}^2$ system. Combinations marked with asterisks are made from the symmetric orbital states.

| | Flavor | Spin | |
|---|---|---|---|
| $A\bar{A}$ | 9 | 0 | $A_{0a}\bar{A}_{0a}{}^*, A_{1a}\bar{A}_{1a}, A_{0s}\bar{A}_{0s}, A_{1s}\bar{A}_{1s}{}^*$ |
| | | 1 | $(A_{0a}\bar{A}_{1a}),(A_{1a}\bar{A}_{0a}), A_{1a}\bar{A}_{1a},(A_{0s}\bar{A}_{1s}),(A_{1s}\bar{A}_{0s}), A_{1s}\bar{A}_{1s}{}^*$ |
| | | 2 | $A_{1a}\bar{A}_{1a}, A_{1s}\bar{A}_{1s}{}^*$ |
| $B\bar{B}$ | 36 | 0 | $B_{0a}\bar{B}_{0a}, B_{1a}\bar{B}_{1a}{}^*, B_{0s}\bar{B}_{0s}{}^*, B_{1s}\bar{B}_{1s}$ |
| | | 1 | $(B_{0a}\bar{B}_{1a}),(B_{1a}\bar{B}_{0a}), B_{1a}\bar{B}_{1a}{}^*,(B_{0s}\bar{B}_{1s}),(B_{1s}\bar{B}_{0s}), B_{1s}\bar{B}_{1s}$ |
| | | 2 | $B_{1a}\bar{B}_{1a}{}^*, B_{1s}\bar{B}_{1s}$ |
| $A\bar{B}$ | 18 | 0 | $(A_{0a}\bar{B}_{0a}),(A_{1a},\bar{B}_{1a}),(A_{0s}\bar{B}_{0s}),(A_{1s}\bar{B}_{1s})$ |
| | | 1 | $A_{0a}\bar{B}_{1a}{}^*, A_{1a}\bar{B}_{0a},(A_{1a}\bar{B}_{1a}), A_{0s}\bar{B}_{1s}, A_{1s}\bar{B}_{0s}{}^*,(A_{1s}\bar{B}_{1s})$ |
| | | 2 | $(A_{1a}\bar{B}_{1a}),(A_{1s}\bar{B}_{1s})$ |

TABLE IV. The relations of the two-meson states to the symmetry classification of the the $q^2\bar{q}^2$ system.

| | $I^G$ | $S$ | Two-meson states |
|---|---|---|---|
| $A\bar{A}$ | $0^+$ | 0 | $PP, VV$ |
| | $0^+$ | 2 | $VV$ |
| | $0^+$ | 1 | $VV$ |
| | $0^-$ | 1 | $PV$ |
| $B\bar{B}$ | $(0,1,2)^+$ | 0 | $PP, VV$ |
| | $(0,1,2)^+$ | 2 | $VV$ |
| | $(0,2)^+$ | 1 | $VV$ |
| | $(0,2)^-$ | 1 | $PV$ |
| | $1^+$ | 1 | $VV, PV$ |
| | $1^-$ | 1 | $VV, PV$ |
| $[A\bar{B}, B\bar{A}]_+$ | $1^+$ | 1 | $VV, PV$ |
| $[A\bar{B}, B\bar{A}]_-$ | $1^-$ | 1 | $VV, PV$ |

antisymmetric component, i.e., $B_{1a}\bar{B}_{1a}$, dominates as is expected from the results for the $A$ scattering in the colored model. The bound-state wave function shown in Fig. 7 clearly shows that the HC component dominates especially at $R>1$ fm and thus the bound state is not a two-mesonlike bound state, as a deuteron for the two-nucleon system, but really a $q^2\bar{q}^2$ state. (3) The phase shift for the model (T) suggests a weak repulsion and the existence of a resonancelike state at around $E=300$ MeV. The coupling with the HC channel is negligible for the phase shift, although the wave function at $E=300$ MeV has a considerable HC component in the inner region. Here we should note that the truncation of the sum in Eq. (2.7) to ground-state mesons effectively eliminates the color van der Waals force in the present RGM calculation. It is expected that the van der Waals force could modify the present results especially at low energies.

The $A\bar{A}$ scattering of two vector mesons with $S=2$ shows very similar features (Fig. 8). For the models (S1) and (T), the two-meson interaction is more attractive than that for the $B\bar{B}$ channel. This is because the color-symmetric state, $|s\rangle$ defined by Eq. (4.8), which is favored in the $A\bar{A}$ system, has less color-octet component than the color-antisymmetric one, $|a\rangle$ by Eq. (4.7), favored in $B\bar{B}$. Because the color-octet component feels strong repulsion for the models (S1) and (T), the $A\bar{A}$ system gets more attraction than $B\bar{B}$. The situation is reversed for the model (S6), where the interaction for $A\bar{A}$ is less attractive than for $B\bar{B}$. In fact, the binding energy in $A\bar{A}$, 262 MeV, is much less than that in $B\bar{B}$. The widths of the resonances seen for the model (S6) are larger than those for $B\bar{B}$, which is again expected by the difference of the color-singlet component between the color-symmetric (4.8) and antisymmetric (4.7) states.

Thus we have obtained several bound and sharp resonance states for large $\rho$, which is expected from the results for the colored model. Those bound and resonance states

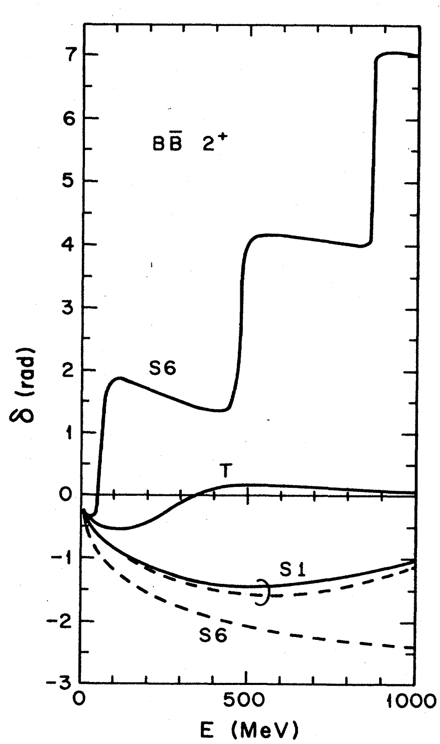


FIG. 6. $B\bar{B}$ scattering phase shifts for $2^+$ ($S=2$, $L=0$). The solid (dashed) curves correspond to the calculation with (without) HC channel coupling. For the model (T), the dashed curve is almost identical to the solid one.

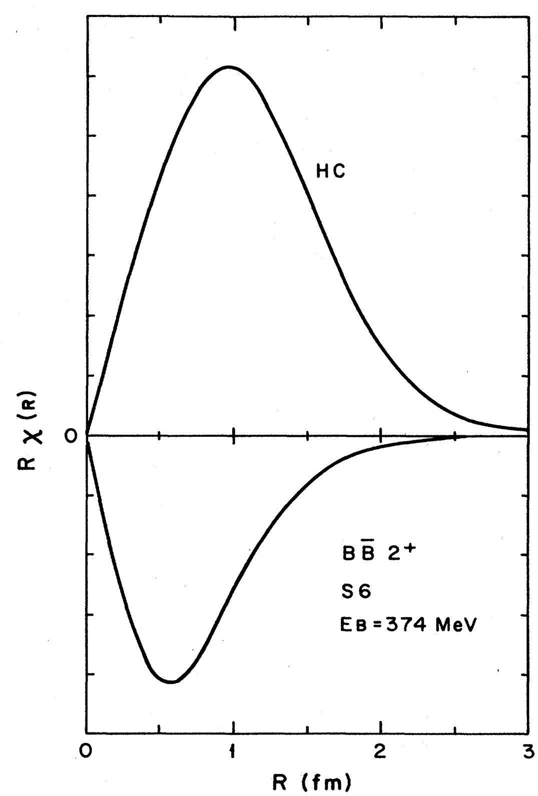


FIG. 7. The relative wave functions of the bound state with the binding energy 374 MeV for the model (S6).

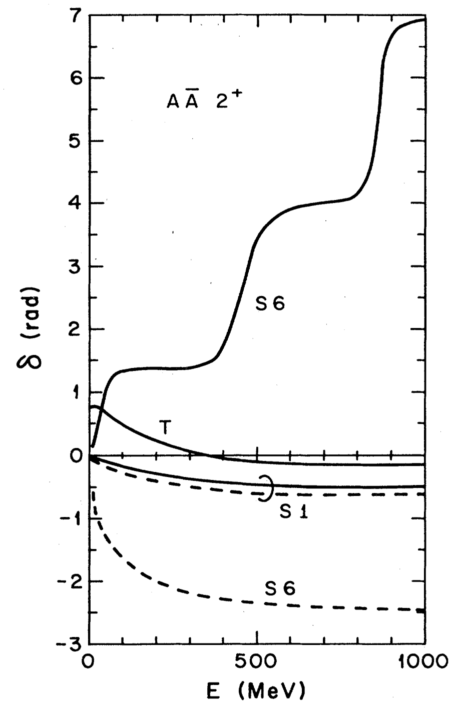


FIG. 8. $2^+$ $A\bar{A}$-scattering phase shifts. See the caption of Fig. 6.

are dominated by HC states, which couple weakly with the two-meson cluster state. The resonances are very sharp ($\Gamma \leq 20$ MeV) because the coupling is very weak. The energies of the bound and resonance states are quite sensitive to the value of the parameter $\rho$, because the contribution of the confining potential to the energy of the HC state is proportional to $1/\sqrt{\rho}$. Figure 9 shows the $\rho$ dependence of the energies of the lowest and second bound or resonance states for the $A\bar{A}$ and $B\bar{B}$ channel. One sees that the energies go up very sharply and the bound state disappears when $\rho$ decreases for $B\bar{B}$, while the $\rho$ dependence is moderate for $A\bar{A}$. As is mentioned above, the eigenchannels with a definite flavor symmetry, $A\bar{A}$ and $B\bar{B}$, are given by the linear combinations (5.4) of the physical two-meson systems, $\rho\rho$ and $\omega\omega$, for $I=0$, while the $(\rho\rho)_{I=2}$ belongs to the $B\bar{B}$ channel. (Note that the $A\bar{A}$ channel has the $I=0$ state only.) The bound and resonance states obtained above may be interpreted in the physical systems as follows. Deeply bound states (binding energy $\geq 300$ MeV) cannot decay into two vector mesons, $VV$, and also are hindered to decay into two pseudoscalar mesons, $PP$, due to the OZI rule. Such states therefore may appear as resonance states with their widths comparable to $\rho$ meson in the meson table. So far there are no candidates for such $2^+$ mesons. The lowest $2^+$ meson is $f(1270)$ ($I^G=0^+$), which is believed to be a member of the $^3P_1$ $q\bar{q}$ nonet.[20] It is therefore unlikely that there exist $2^+$ deeply bound states of two vector mesons. It gives a condition, $\rho < 5$.

Shallow bound states, however, can decay into $\rho\rho$ due to the large width of the $\rho$ meson, but not into $\omega\omega$. The $I=0$ states in the $B\bar{B}$ channel couples mainly with $(\rho\rho)_{I=0}$ [see Eq. (5.4)] and have a degenerate partner with $I=2$, which couples only with $(\rho\rho)_{I=2}$. On the other hand, the $I=0$ states in the $A\bar{A}$ channel couples mainly with $\omega\omega$. One can expect that the $2^+$ $B\bar{B}$ states with $I=0$ and $I=2$ come out as $\rho\rho$ ($4\pi$) resonances around threshold if $\rho \simeq 2$–4. The $I=0$ $2^+$ $A\bar{A}$ state will also appear as an $\omega\omega$ ($6\pi$) bound or resonance state for $\rho \geq 2$.

Such $q^2\bar{q}^2$ states have been investigated as discrete states in the MIT bag model by Jaffe[18] and were adopted to analyze recent experimental data,[21] $\gamma\gamma \to \rho\rho$ and $J/\psi \to \gamma VV$. According to Ref. 21, three $2^+$ resonances at around $E=100$ MeV in the ($A\bar{A}$, $I=0$) and ($B\bar{B}$, $I=0$ and 2) can reproduce the strong enhancement of $\gamma\gamma \to \rho^0\rho^0$ observed. If $\rho=2$–3 with the parameter set (I), we find that the resonance spectrum obtained here is similar to that for the MIT bag model. The resonance states obtained here, however, have a much larger branching ratio to the HC state than that for the MIT bag model, where the branching ratio is determined only by kinematical recoupling coefficients. We have a dynamical enhancement of the HC state for large $\rho$. The smallness of the coupling with the ordinary two-meson states gives the resonances very small widths.

The $I=0$ resonance states can be treated from two-gluon states because of the large HC component. They also mix the glueball state with $J^P=0^+$ or $2^+$ ($S$-wave two-gluon bound states).[22] Recent reports of the radiative $J/\psi$ decays into two vector mesons ($J/\psi \to \gamma VV$)[23] show interesting structures around $\sqrt{s}=1.6$ GeV. For $J/\psi \to \gamma\rho\rho$, $2^+$ enhancement is seen besides the large $0^-$ contribution. It is also suggested[24] that the $2^+$ state could be different from another $2^+$ state $\theta(1640)$ observed in $J/\psi \to \gamma\eta\eta$ and $J/\psi \to \gamma K\bar{K}$. If it is true, we may expect that the two $2^+$ states in the same region are two orthogonal linear combinations of the $2^+$ glueball and the $I=0$ $B\bar{B}$ $q^2\bar{q}^2$ state.

Next we consider $0^+$ $K\bar{K}$ scattering. Several people have discussed the possibility that the resonance $S^*(975)$ and $\delta(980)$ are $K\bar{K}$ bound states (or $q^2\bar{q}^2$).[18,19,3] Here we

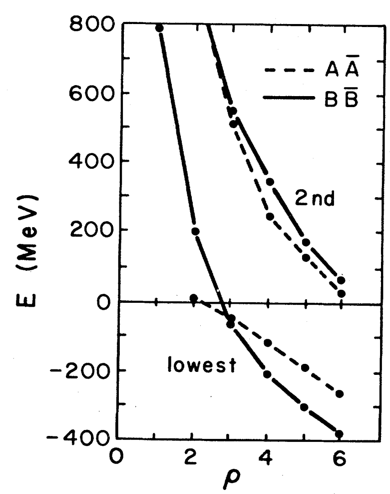


FIG. 9. $\rho$-parameter dependence of the lowest and the second bound or resonance energies. The solid (dashed) curves show the energies of the $B\bar{B}$ ($A\bar{A}$) $2^+$ states.

wish to apply the present model to the $K\bar{K}$ system and examine the existence of bound and low-energy resonance states. The $K\bar{K}$ system contains a strange quark and a strange antiquark. Because the strange quark is heavier than the $u$ and $d$ quarks, the kinetic energy term of the Hamiltonian cannot be expressed by as simple a form as Eq. (2.4), which makes the problem too complicated. Here we simply take a system where all the particles have the same mass,

$$m_q = [(1/m_{u,d} + 1/m_s)/2]^{-1} = 375 \text{ MeV} ,$$

in order to avoid the complexity mentioned above.[25] This approximation does not affect the single-meson spectrum obtained, because the interaction is taken independent of the quark mass. The corresponding excitation energy of the harmonic oscillator, $\hbar\omega$, is 450 MeV.

Several channels will couple with $K\bar{K}$, such as $\eta_0\eta_s$, $K^*\bar{K}^*$,$\omega\phi$ or $\rho\phi$. Again the flavor degeneracy tells us that for each flavor-symmetry state, i.e., $A\bar{A}$ or $B\bar{B}$, channels of two pseudoscalar mesons ($PP$) and of two vector mesons ($VV$) are relevant. The unitary transformation between the physical channels and the flavor-symmetric ones is given by

$$\begin{bmatrix} A\bar{A} \\ B\bar{B} \end{bmatrix} = \begin{bmatrix} 1/\sqrt{2} & \pm 1/\sqrt{2} \\ 1/\sqrt{2} & \mp 1/\sqrt{2} \end{bmatrix} \begin{bmatrix} M_0 M_{s\bar{s}} \\ M_s M_{\bar{s}} \end{bmatrix} , \tag{5.5}$$

where the upper (lower) sign gives the transformation for $I=0$ (1) and $M_0$, $M_s$, $M_{\bar{s}}$, and $M_{s\bar{s}}$ stand for the meson with no strange quark, with $s$, with $\bar{s}$, and with $s\bar{s}$, respectively. One can easily see that for the low-lying $q^2\bar{q}^2$ states the $A\bar{A}$ flavor-symmetric state has lower energy than the $B\bar{B}$ state due to the color-magnetic interaction.[18] In fact, the $0^+$ $A_{0a}\bar{A}_{0a}$ state feels strong color-magnetic attraction and becomes the lowest $q^2\bar{q}^2$ state. The $K$-$\bar{K}$ interaction for the $A\bar{A}$ symmetry is investigated to examine the lowest $K$-$\bar{K}$ bound or resonance state. Because we expect the HC state to be important, we have a coupled-channel problem with four channels $PP$, $VV$, $P_8P_8$, and $V_8V_8$.

Figure 10 shows the $A\bar{A}$ scattering phase shifts for the three models, (T), (S1), and (S6). One sees very similar curves as for the $2^+$ channel. The models (S6) and (T) have bound states, whose binding energies are 67 MeV and $\sim$0 MeV, respectively. It is found from the bound-state wave function that the $V_8V_8$ channel couples most strongly in the bound state of the model (S6), because the color-magnetic interaction gives lower energy to $V_8V_8$ than the other excited channels, $VV$ and $P_8P_8$. For the models (S1) and (T), the effect of the channel coupling is small and no resonancelike structure is seen.

The quark mass $m_q$ and $\rho$ dependence of the lowest bound-state energy is illustrated in Fig. 11. One sees that the $\rho$ dependence is much weaker than for the $2^+$ $VV$ state energies (Fig. 9). The mass dependence is almost negligible especially for large $\rho$. One can conclude that two $K\bar{K}$ bound states ($I=0$ and 1) with the binding energy of a few tens MeV are predicted for the string-flip model with $\rho \geq 3$. The $M_0M_{s\bar{s}}$ system, i.e., $\pi\eta_s$ or $\eta_0\eta_s$,

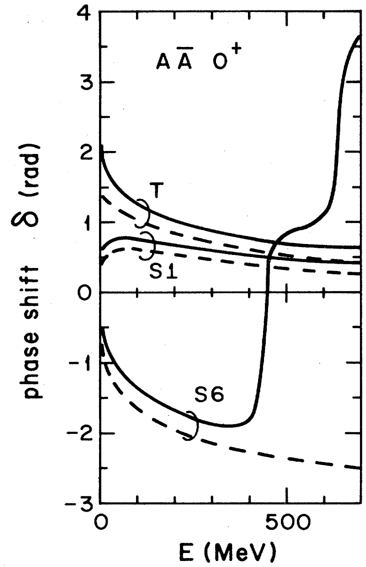


FIG. 10. $K\bar{K}$ $0^+$ scattering phase shifts in the $A\bar{A}$ flavor symmetry. The solid (dashed) curves correspond to the calculation with (without) channel coupling with $VV$, $P_8P_8$, and $V_8V_8$.

couples to the bound state as is known from Eq. (5.5), while the decay into two nonstrange mesons, such as $\pi\pi$, $\eta_0\pi$, and $\eta_0\eta_0$, is suppressed due to the OZI rule. We therefore expect the states to be clearly observed as sharp meson resonances.

Weinstein and Isgur[3] investigated the two-meson system in the two-body potential model of confinement. They claimed that the $K\bar{K}$ system has a very shallow $S$-wave bound state, which may be the $S^*(975)$ ($I=0$) and $\delta(980)$ ($I=1$). Our calculation for the model (T) seems consistent with theirs. We wish to stress here that the bound state obtained for the string-flip model has completely different features from those of the bound state obtained for the model (T). The HC coupling is negligibly weak for the two-body potential model, while the bound state for a large $\rho$ is dominated by the HC component.

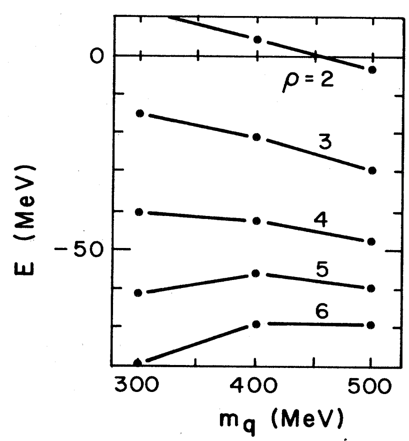


FIG. 11. The quark-mass ($m_q$) dependence of the lowest $0^+$ bound-state energy for several values of $\rho$.

Another calculation with the two-body confining potential[4] showed that energies of HC discrete levels are much higher than the $VV$ threshold. This is consistent with the smallness of the HC component observed here for the model (T).

When we assume that the $S^*$ ($I=0$) resonance is a $K\bar{K}$ bound state with large HC component, the mixing with the $0^+$ glueball is to be considered. It was also suggested[20,26] that the $S^*$ and $\delta$ are mixed states of $q\bar{q}$ and $q^2\bar{q}^2$. To answer the question, which component is most important, we will need a more careful analysis of the experimental data, which is not the purpose of this paper.

As a summary of the calculations in the realistic model, we present several general features obtained here: (1) The strong $\rho$ dependence observed in the colored string-flip model is preserved. For small $\rho$ ($\rho \leq 2$), the effect of the HC coupling is negligible and generally the meson-meson interaction is weakly repulsive. On the other hand, a bound state and several sharp resonances appear for large $\rho$ ($\rho \geq 3$), which are dominated by a HC confined component. Resonance widths vary from several MeV to a few hundred MeV. (2) The two-body potential model of confinement shows quite different features from the string-flip model for the meson-meson interaction. It usually gives a moderate attraction and the contribution of HC states is very weak. The bound states obtained are deuteronlike two-meson states, where HC plays no significant role. It should be noted that the color van der Waals force, which was avoided by neglecting the internal excitations of the mesons, may change the above results significantly.

## VI. CONCLUSION

The two-meson system is the simplest multihadron system, which provides us with a good place to test the potential quark model. We have applied the string-flip model of quark confinement to the two-meson or $q^2\bar{q}^2$ system without any internal degrees of freedom (colorless model), with color (colored model), and with color, spin, and flavor (realistic model). We have a free parameter $\rho$, which cannot be fixed by the single-meson spectrum, when we take account of color. We observed a rich structure for a large value of $\rho$ in two-meson spectrum. The bound states and the sharp resonances are found to come from the coupling with hidden-color confined states and therefore are a quite new kind of multiquark system never seen before. In fact, we predict the $I^G=0^+$ and $1^-$ $K\bar{K}$ bound states with a binding energy of a few tens of MeV, which might be assigned as $S^*(975)$ and $\delta(980)$ resonances. We also predict that the two-vector-meson system with ($S=2$, $L=0$) may have several bound or sharp low-lying resonance states. The energies of the states are strongly dependent on the parameter $\rho$. Clear observation of such $2^+$ states an fix the value of $\rho$. So far $\rho \simeq 3$—$4$ is preferable if we assume that the $2^+$ resonances around 1.6 GeV and $S^*$ and $\delta$ come mainly from the coupling with the $q^2\bar{q}^2$ hidden-color states.

The final comment is devoted to other possible choices of the confining potential. The colored confining potential employed here is one of the simplest extensions of the original string-flip model without color. The color projection operator is introduced to confine color-nonsinglet states, while color-singlet subsystems can come out as free particles. However, we may consider other prescriptions to take the color into account. One of them is the introduction of a $qq$ or $\overline{qq}$ confining force for hidden-color states, which requires an extra free parameter in the colored confining potential. A particular choice of the new parameter taken in Ref. 8 leads to a model where the $x$ coordinate decouples completely. We see that the results in Ref. 8 are qualitatively similar to ours in two-meson systems.

When we apply the string-flip model to a multibaryon system, we may consider possible form for the colored confining potential, where the string potential acts only on pure color-singlet three-quark systems. The model shows quite different features in two-baryon systems[27] and is also applicable to many-quark systems,[28] where the model with color projection operators is hard to apply.

## ACKNOWLEDGMENTS

The author would like to thank E. J. Moniz for suggesting the present problem and for many fruitful suggestions and discussions. He also thanks C. J. Horowitz for discussions and careful reading of the manuscript and K. F. Liu and K. Yazaki for useful discussions. This work was supported in part through funds provided by the U.S. Department of Energy (DOE) under Contract No. DE-AC02-76ERO3069.

[1]E. Eichten *et al.*, Phys. Rev. Lett. **34**, 369 (1975); Phys. Rev. D **17**, 3090 (1978); **21**, 203 (1980); C. Quigg and J. L. Rosner, Phys. Lett. **71B**, 153 (1977); K. F. Liu and C. W. Wong, *ibid.* **73B**, 223 (1978); Phys. Rev. D **17**, 2350 (1978); W. Celmaster, H. Georgi, and M. Machacek, *ibid.* **17**, 879 (1978).

[2]A. De Rújula, H. Georgi, and S. L. Glashow, Phys. Rev. D **12**, 147 (1975); D. Gromes and I. Stamatescu, Nucl. Phys. **B112**, 213 (1976); W. Celmaster, Phys. Rev. D **15**, 1391 (1977); N. Isgur and G. Karl, Phys. Lett. **72B**, 109 (1977); Phys. Rev. D **18**, 4187 (1978); **19**, 2653 (1979); **20**, 1191 (1979); R. K. Bhaduri, L. E. Cohler, and Y. Nogami, Phys. Rev. Lett. **44**, 1369 (1980); S. Ono and F. Schöberl, Phys. Lett. **118B**, 419 (1982); A. J. G. Hey and R. L. Kelly, Phys. Rep. **96**, 71 (1983).

[3]J. Weinstein and N. Isgur, Phys. Rev. Lett. **48**, 659 (1982); Phys. Rev. D **27**, 588 (1983).

[4]R. Aaron and M. H. Friedman, Phys. Rev. D **25**, 1964 (1982); R. Aaron, M. H. Friedman, and C. P. Jargocki, *ibid.* **28**, 1783 (1983).

[5]D. A. Liberman, Phys. Rev. D **26**, 3039 (1982); J. E. T. Ribeiro, Z. Phys. C **5**, 27 (1980); M. Oka and K. Yazaki, Phys. Lett. **90B**, 41 (1980); Prog. Theor. Phys. **66**, 556 (1981); **66**, 572 (1981); Nucl. Phys. **A402**, 477 (1983); M. Harvey, *ibid.* **A352**, 326 (1981); M. Harvey, J. Letourneux, and B. Lorazo, *ibid.* **A424**, 428 (1984); A. F. Faessler, F. Fernandez, C.

Lübeck, and K. Shimizu, Phys. Lett. **112B**, 201 (1982); Nucl. Phys. **A402**, 555 (1983); K. Maltman and N. Isgur, Phys. Rev. Lett. **50**, 1827 (1983); Phys. Rev. D **29**, 952 (1984); M. Oka and K. Yazaki, in *Quarks and Nuclei,* edited by W. Weise (World Scientific, Singapore, 1985).

[6]H. J. Lipkin, Phys. Lett. **45B**, 267 (1973); N. Isgur, in *The New Aspects of Subnuclear Physics,* proceedings of the XVI International School of Subnuclear Physics, Erice, 1978, edited by A. Zichichi (Plenum, New York, 1980).

[7]P. M. Fishbane and M. T. Grisaru, Phys. Lett. **74B**, 98 (1978); T. Appelquist and W. Fischler, *ibid.* **77B**, 405 (1978); R. S. Willey, Phys. Rev. D **18**, 270 (1978); S. Matsuyama and H. Miyazawa, Prog. Theor. Phys. **61**, 942 (1978); M. B. Gavella *et al.*, Phys. Lett. **82B**, 431 (1979); G. Feinberg and J. Sucher, Phys. Rev. D **20**, 1717 (1979); K. F. Liu, Phys. Lett. **131B**, 195 (1983).

[8]F. Lenz, J. T. Londergan, E. J. Moniz, R. Rosenfelder, M. Stingl, and K. Yazaki (in preparation); K. Yazaki, Nucl. Phys. **A416**, 87c (1984); J. T. Londergan, in *Hadron Substructure in Nuclear Physics,* proceedings of the Workshop, University of Indiana, 1983, edited by W. Y. P. Hwang and M. H. Macfarlane (AIP, New York, 1983).

[9]K. Johnson and C. B. Thorn, Phys. Rev. D **13**, 1934 (1976); R. E. Cutkosky and R. E. Hendrick, *ibid.* **16**, 786, (1977); **16**, 793 (1977); J. Carlson, J. Kogut, and V. R. Pandharipande, *ibid.* **27**, 233 (1983); **28**, 2807 (1983); N. Isgur and J. Paton, Phys. Lett. **124B**, 247 (1983).

[10]J. A. Wheeler, Phys. Rev. **32**, 1083 (1937); **32**, 1107 (1937); K. Wildermuth and Th. Kanellopoulos, Nucl. Phys. **7**, 150 (1958); I. Shimodaya, R. Tamagaki, and H. Tanaka, Prog.

[11]M. Kamimura, Prog. Theor. Phys. Suppl. **62**, 236 (1977) and references therein.

[12]The role of the Pauli-forbidden state in the scattering of two composite particles is well known, for instance, for $\alpha$-$\alpha$ scattering: R. Tamagaki and H. Tanaka, Prog. Theor. Phys. **34**, 191 (1965); S. Okai and S. C. Park, Phys. Rev. **145**, 787 (1966); also see M. Oka and K. Yazaki, Prog. Theor. Phys. **66**, 556 (1981); **66**, 572 (1981); in *Quarks and Nuclei* (Ref. 5) for baryon-baryon cases.

[13]The proof is similar to that for the six-quark system given by M. Oka and K. Yazaki, in *Quarks and Nuclei* (Ref. 5).

[14]M. Harvey, Nucl. Phys. **A352**, 301(1981); **A352**, 326 (1981).

[15]A series of the zero-width resonances is expected for $\rho=2$, because the $x$ coordinate is decoupled again. It cannot affect the scattering phase shifts obtained here.

[16]As was discussed in Sec. II, the convergence of the expansion may be very slow for the two-body potential model due to the color van der Waals force. Here we do not repeat the argument on this problem.

[17]The importance of this procedure in the study of two-composite-particle systems has been shown for the two-nucleon system by S. Ohta, M. Oka, A. Arima, and K. Yazaki, Phys. Lett. **119B**, 35 (1982).

[18]R. L. Jaffe, Phys. Rev. D **15**, 267 (1977); **15**, 281 (1977).

[19]F. Close, *An Introduction to Quarks and Partons* (Academic, New York, 1979), p. 430.

[20]Particle Data Group, Rev. Mod. Phys. **56**, S1 (1984).

[21]N. N. Achasov, S. A. Devyanin, and G. N. Shestakov, Phys. Lett. **108B**, 134 (1982); Z. Phys. C **16**, 55 (1982); B. A. Li and K. F. Liu, Phys. Lett. **118B**, 435 (1982); Phys. Rev. Lett. **51**, 1510 (1983); Phys. Rev. D **30**, 613 (1984); H. Kolanoski, in *Proceedings of the Fifth International Workshop on Photon-Photon Collisions, Aachen,* edited by Ch. Berger (Springer, Berlin, 1983), p. 175.

[22]Theoretical predictions of the spin-parity and mass of glueballs and experimental situations are summarized by S. Meshkov, in *Experimental Meson Spectroscropy—1983,* proceedings of the Seventh International Conference, Brookhaven, edited by S. J. Lindenbaum (AIP, New York, 1984).

[23]N. Wermes, in *Proceedings of the XIXth Rencontre de Moriond, La Plagne, France, 1984,* edited by J. Tran Thanh Van (Éditions Frontières, Gif-sur-Yyette, 1984).

[24]B. A. Li and K. F. Liu, Phys. Rev. D **30**, 613 (1984).

[25]The mass is taken as the reduced mass so that the kinetic-energy term of the single-meson Hamiltonian remains unchanged. Note that the rest-mass term of the Hamiltonian gives a constant shift to the energy of the system, which affects neither the meson spectrum nor the meson-meson interaction.

[26]N. A. Törnqvist, Phys. Rev. Lett. **49**, 624 (1982); L. Montanet, Rep. Prog. Phys. **46**, 337 (1983).

[27]M. Oka and C. J. Horowitz, Phys. Rev. D (to be published).

[28]C. J. Horowitz, in *Hadron Substructure in Nuclear Physics* (Ref. 8); C. J. Horowitz and R. Panoff, Talk presented at the conference in *Intersections Between Nuclear and Particle Physics,* in proceedings of the Conference, Steamboat Springs, Colorado, 1984, edited by R. Mischke (AIP, New York, 1984); C. J. Horowitz, E. J. Moniz, and J. W. Negele, Phys. Rev. D **31**, 1689 (1985).